

# Chemical Science

Accepted Manuscript

This article can be cited before page numbers have been issued, to do this please use: L. Michel, V. Steinmetz, S. Godel-Pastre, P. Durand and A. Chevalier, *Chem. Sci.*, 2025, DOI: 10.1039/D5SC03665H.



This is an Accepted Manuscript, which has been through the Royal Society of Chemistry peer review process and has been accepted for publication.

Accepted Manuscripts are published online shortly after acceptance, before technical editing, formatting and proof reading. Using this free service, authors can make their results available to the community, in citable form, before we publish the edited article. We will replace this Accepted Manuscript with the edited and formatted Advance Article as soon as it is available.

You can find more information about Accepted Manuscripts in the [Information for Authors](#).

Please note that technical editing may introduce minor changes to the text and/or graphics, which may alter content. The journal's standard [Terms & Conditions](#) and the [Ethical guidelines](#) still apply. In no event shall the Royal Society of Chemistry be held responsible for any errors or omissions in this Accepted Manuscript or any consequences arising from the use of any information it contains.

## ARTICLE

## A Mitochondria Targeted Nitroreductase-Sensitive Self-Immolative Spacer as Efficient Shuttle for Uncharged Amine-Based Molecules.

Laurane Michel,<sup>a</sup> Vincent Steinmetz,<sup>a</sup> Sophia Godel-Pastre,<sup>a</sup> Philippe Durand,<sup>a</sup> and Arnaud Chevalier<sup>\*a</sup>Received 00th January 20xx,  
Accepted 00th January 20xx

DOI: 10.1039/x0xx00000x

Mitochondria have emerged as critical therapeutic targets in a wide range of diseases. The detailed examination of this organelle, as well as the search for methods to efficiently address it, therefore, represent significant challenges. In this article, we present a simple and robust method for the functionalization of uncharged amine-based molecules to enable their intracellular transport and selective accumulation in mitochondria. To this end, we have synthesized a self-immolative spacer that is both sensitive to mitochondrial nitroreductase and incorporates a triphenylphosphonium vectorising moiety. To demonstrate the efficacy of this mitochondrial shuttling technology, we have designed, synthesized, and employed a fluorogenic probe that unambiguously validates the concept. An initial extension of this technology for therapeutic purposes is proposed through the intramitochondrial delivery of native doxorubicin, showing promising potential to overcome drug resistance mechanisms.

## Introduction

In addition to its role as the energy powerhouse of the cell, mitochondrion is involved in the control of several cellular processes. Its dysfunction is thus connected to numerous pathologies,<sup>1</sup> such as cancers<sup>2</sup> and neurodegenerative diseases,<sup>3</sup> but also overweight-related diseases such as diabetes<sup>4</sup> and non-alcoholic fatty liver.<sup>5</sup> Very recently, mitochondrial respiratory complex IV deficiency has been identified as a potential contributor to amyotrophic lateral sclerosis (ALS),<sup>6</sup> a severe neurodegenerative disease, further expanding the growing list of pathologies linked to mitochondrial dysfunction. Mitochondria thus emerge as a highly relevant biological target, fully justifying the development of innovative chemical tools to probe their functions and modulate their activity. The physicochemical properties that confer on a molecule the propensity to penetrate mitochondria are reasonably well understood. Murphy demonstrated the ability of lipophilic cations to cross the polarized double membrane of mitochondria efficiently.<sup>7</sup> As a result, numerous molecular entities, so-called mitochondriotropic, have emerged in recent years.<sup>8</sup> Their conjugation to a molecule of interest is a strategy for vectorizing the latter into mitochondria, triphenylphosphonium (TPP) being the preferred mitochondriotropic moiety.<sup>9</sup> In this context, various strategies have been developed to prepare

mitochondria-targeted analogues of existing probes or drugs. These derivatives, incorporate structural modifications, involving mitochondriotropic moiety, that enable their selective accumulation in mitochondria, thereby facilitating the visualization and study of mitochondrial structure and activity.<sup>8–10</sup> The aim may be either diagnostic by observing intramitochondrial biochemical processes,<sup>11</sup> or therapeutic<sup>12</sup> by addressing active compounds. However, almost all such conjugates have been formed through the formation of an irreversible linkage between the two entities. To our knowledge, except a few techniques involving encapsulation in nanostructures coated with mito-targeting groups (mitoNANO), there is only a few implementable technologies allowing both the transport and controlled release of active molecules within the mitochondria.<sup>13</sup>

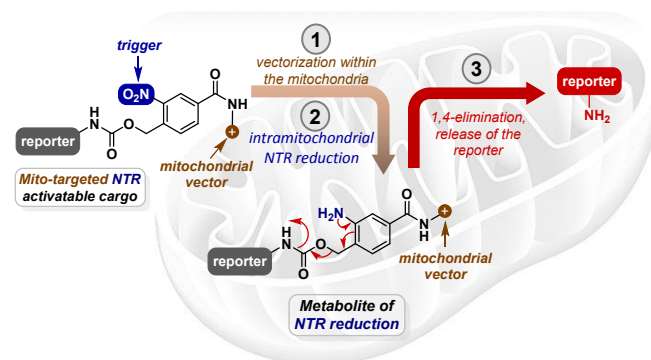


**Figure 1.** Concept of “mitochondrial shuttling” using mito-targeted SIS activatable by mitochondrial NTR.

The reported mitochondria-targeted prodrugs are activated by photoactivation,<sup>14</sup> GSH,<sup>15</sup> ROS,<sup>16</sup> or carboxylesterase,<sup>17</sup> which

<sup>a</sup> Université Paris-Saclay, CNRS, Institut de Chimie des Substances Naturelles, UPR 2301, 91198, Gif-sur-Yvette, France.

\*Electronic Supplementary Information (ESI) available: See DOI: 10.1039/x0xx00000x



are also prevalent outside the mitochondria and can thus lead to non-specific release. This study was motivated by the design of a mitochondria-targeted activatable platform responsive to mitochondrial-specific enzymatic activity. Such a system enables the functionalization of uncharged molecules of interest (probe and/or drugs), facilitating their targeted delivery to mitochondria and subsequent controlled release via an intracellular shuttling process (Figure 1). For this, reductases are relevant activators. Reductases are key enzymatic markers of hypoxic environments, widely exploited for diagnostic imaging<sup>18</sup> and prodrug activation.<sup>19</sup> Beyond their well-established role under low oxygen levels, recent evidence highlights their significant activity within mitochondria even under normoxic conditions. In this organelle, reductases contribute critically to maintaining redox balance, thus ensuring mitochondrial homeostasis and supporting essential bioenergetic functions.<sup>20</sup> This dual behavior underscores their value as both biological targets and tools for selective activation strategies within the mitochondrial microenvironment. Indeed, their selective activity within mitochondria under normoxic conditions confers a level of specificity that surpasses that of more commonly investigated biomarkers such as carboxylesterases, reactive oxygen species (ROS), or glutathione (GSH), which often lack subcellular selectivity. During the last decade, the use of fluorogenic probes have enabled the visualization of some of these intramitochondrial redox enzymes, such as thioredoxin reductases,<sup>21</sup> nitroreductase (NTR),<sup>22</sup> quinone reductases (NQOs),<sup>23</sup> methionine reductases (MSr)<sup>24</sup> and more recently azoreductase (AzoR).<sup>25</sup> Despite the diagnostic potential of these reductases, their use in a therapeutic context remains largely underexplored. It seems nonetheless obvious that they can be strategically leveraged to activate prodrugs through a controlled mitochondrial release mechanism. In this work, we introduce a novel concept: the design and synthesis of a nitroreductase-activated self-immolative spacer (SIS) bearing a triphenylphosphonium (TPP) targeting group. This SIS system enables the targeted delivery and controlled release of uncharged amine-containing molecules, including potential therapeutic agents, specifically within the mitochondria. This approach features a new paradigm in intracellular drug delivery, here called "mitochondrial shuttling" (Figure 1). This strategy goes beyond passive covalent and permanent targeting approaches by using enzyme-triggered activation to achieve spatiotemporal control, thus marking a step forward in mitochondrial-controlled release. To our knowledge, this strategy is the first method using specific mitochondrial enzymatic activity for shuttling neutral molecules into mitochondria.

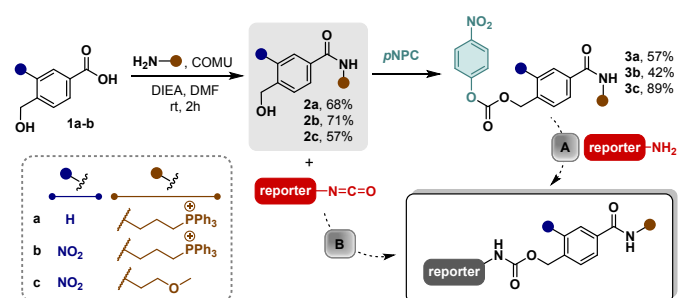
## Results and Discussions

### Design and Synthesis mito-targeted SIS activatable by mitochondrial NTR.

As illustrated in Scheme 1, the design of this self-immolative spacer (SIS) combines a mitochondriotropic triphenylphosphonium (TPP) unit with a nitro-activatable group

strategically positioned *ortho* to a benzylic alcohol. This configuration enables subsequent acylation to form carbamates from amine-based molecules of interest. To access these compounds, we developed a divergent strategy from benzylic alcohols **2a-c**, relying on two complementary approaches (routes A and B) designed to accommodate both aromatic and aliphatic amines, which differ in their nucleophilicity. Here, the route A involves the addition of a nucleophilic amine to a nitrophenyl carbonate (**3a-c**), while route B exploits the addition of alcohol onto an isocyanate as an activated form of less nucleophilic aniline. To enable a comprehensive study, we synthesized three analogues of each benzylic alcohol.

**Scheme 1.** Synthesis of mito-targeted NTR activatable SIS and illustration of potential use for the preparation of mito-targeted probes and/or prodrugs



Compound **2a** lacks the nitro group and will serve for the synthesis of mitochondria-targeted compounds that are not activatable by nitroreductase (unactivatable control molecules). The 2-methoxy-ethyl benzamide **2c**, on the other hand, allows the generation of NTR-activatable compounds, that are not targeted to mitochondria, thereby helping to confirm the organelle selectivity of the activation process. Finally, alcohol **2b** combines both the TPP moiety and the nitro group, enabling both mitochondrial targeting and triggered release of the molecule of interest. These *para*-hydroxymethyl benzamide **2a-c** were obtained from the corresponding benzoates (**1a-b**) by an amidation reaction with amines using oxyma-based COMU as coupling agent. The reaction with TPP carrying propyl amine led to alcohols **2a** and **2b** in 68% and 71% yield, respectively while reaction with 2-methoxy-ethylamine led to compound **2c** in 57% yield. All the alcohols **2a-c** thus obtained were then converted to the corresponding nitrophenyl carbonates **3a-c** by reaction with *para*-nitrophenyl chloroformate (pNPC). All these intermediates demonstrated sufficient stability to be stored for several months under inert atmosphere at low temperature, making them valuable and versatile tools for the single-step functionalization of a broad range of amines.

### Synthesis and *in vitro* study of a fluorogenic probe incorporating the mito-targeted SIS activatable by NTR.

To demonstrate the effectiveness of the shuttling process, we first used fluorescent amines that could be easily observed in cells. This fluorescent reporter was chosen to easily differentiate it from its acylated form, allowing us to confirm that the release of the reporter had occurred. To this end, 4-amino-1,8-naphthalimide (**4-ANI**) was selected as a suitable



candidate due to its well-established fluorescent properties and compatibility with acylation strategies. This fluorophore is commonly used to engineer suitable probes for fluorescence

microscopy<sup>26</sup> including ratiometric probes.<sup>27</sup> Probes **5a-c** were synthesized using route B from alcohols **2a-c** and isocyanate **4**, produced *in situ* by reacting **4-ANI** with triphosgene (Figure 2a).

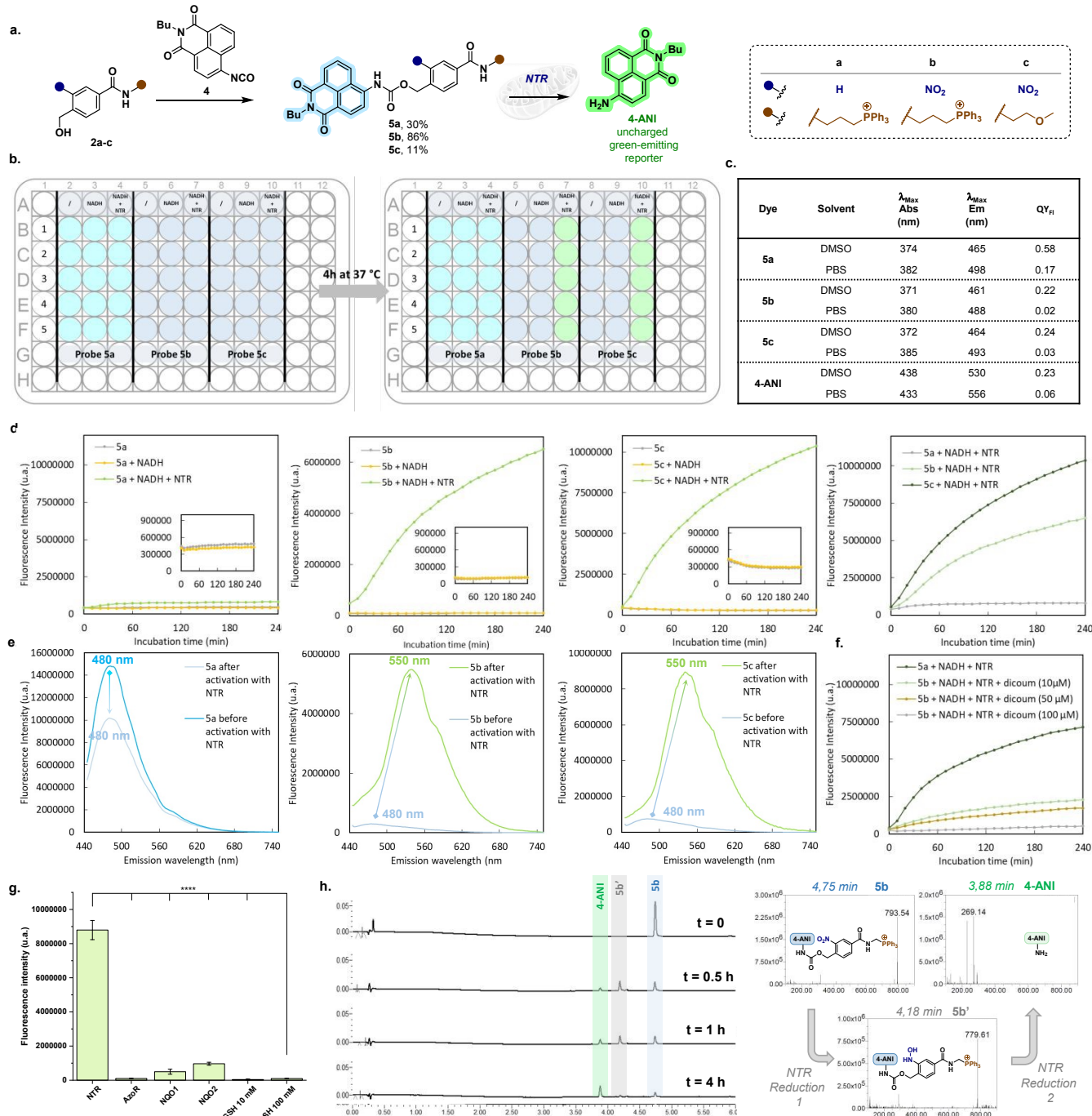


**Figure 2. Synthesis, photophysical characterization and *in vitro* enzymatic conversion of ratiometric fluorogenic probe **5a-c**.** **a.** Synthesis of a 4-ANI-based fluorogenic probe (**5a-c**) and principle of ratiometric response to NTR. **b.** Schematic representation of a 96-well plate illustrating the fluorescence emission color change associated with the release of **4-ANI** following the enzymatic activation of probes **5a-c**. **c.** Photophysical properties of probes **5a-c** and **4-ANI** measured in PBS buffer and DMSO at 25 °C. Relative  $QY_F$  were calculated using Quinine Sulfate ( $QY_F = 0.59$  in  $HClO_4$  0.1M)<sup>28</sup> for probes **5a-c** or Coumarin 153 ( $QY_F = 0.53$  in EtOH)<sup>28</sup> for **4-ANI**. **d.** Kinetic monitoring of NTR activation (1  $\mu$ g) of probes **5a-c** (10  $\mu$ M in PB buffer pH = 7.4 + NADH 500  $\mu$ M). The fluorescence was recorded over time at 540 nm with excitation fixed at 435 nm. **e.** Emission spectra of probes **5a-c** upon excitation at 405 nm recorded before and after incubation for 4h with NTR in presence of NADH (500  $\mu$ M). **f.** Inhibition effect of dicoumarol on **5b** activation by NTR (fluorescence was recorded over time at 540 nm with excitation fixed at 430 nm). **g.** Comparison of fluorescence intensity recorded after 30 min of incubation with multiple reducing agents at 37 °C. **h.** UHPLC/MS analysis of the NTR-mediated transformation of probe **5c**, giving the corresponding fluorophore **4-ANI** through the hydroxylamine intermediate **5b'** and corresponding MS spectra.

Absorbance and fluorescence measurements were carried out in DMSO and PBS, and the results are shown in table Figure 2c

(detailed photophysical properties are available in Table S1 and Figures S1 to S3). They confirm that probes **5a-c** exhibit blue





emission centered around 465 nm in DMSO and 490 nm in PBS. These emissions are readily distinguishable from the green emission of the expected released fluorophore, **4-ANI**, which displays maxima at 530 nm and 556 nm, respectively. Notably, the fluorescence quantum yields ( $QY_F$ ) of probes **5b** and **5c** were significantly lower than **5a**, likely due to photo-induced electron transfer (PeT) quenching effect arising from the nitro moiety. To assess whether the probes **5b** and **5c** could be enzymatically activated by NTR and promote the release of **4-ANI**, *in vitro* studies were performed using a commercially available enzyme. Each probe was incubated in phosphate buffer (pH 7.5) containing 1% DMSO at 37 °C. For each compound, three conditions were tested: incubation alone, with NADH, and with both NADH and NTR. Fluorescence was monitored over 4 hours using a plate reader, with each experiment performed in quintuplicate (Figure 2b). Emission spectra were recorded before and after enzymatic activation for all probes. The release of **4-ANI** was monitored by tracking the increase in its green fluorescence at 540 nm over time, upon excitation at 435 nm (Figure 2d). For each probe, no significant change in fluorescence was observed when incubated alone or in the presence of 500  $\mu$ M NADH, confirming their stability under the experimental conditions. In contrast, a marked fluorescence increase was detected for both nitro functionalized probes **5b** and **5c** upon incubation with NTR, suggesting successful activation *via* nitro group reduction followed by the release of **4-ANI**. This was further supported by the absence of fluorescence increase for probe **5a**, which lacks the nitro-activatable moiety. Comparison of fluorescence kinetics (Figure 2d, right, Fig S5) indicates that probe **5c** ( $K_m = 2.72 \mu$ M,  $V_{max} = 702 \text{ cps} \cdot \text{s}^{-1} \cdot \text{min}$ ) is activated more rapidly than **5b** ( $K_m = 1.98 \mu$ M,  $V_{max} = 566 \text{ cps} \cdot \text{s}^{-1}$ ), likely due to reduced steric hindrance in the absence of the TPP moiety, which may obstruct enzyme accessibility. These findings were corroborated by emission spectra recorded before and after NTR activation (Figure 2e). While probe **5a** showed no spectral shift, probes **5b** and **5c** exhibited a clear red shift and a pronounced fluorescence enhancement, consistent with the release of free **4-ANI**. Additionally, the fluorescence increases at 540 nm observed upon incubation of probe **5b** with NTR was progressively attenuated in the presence of increasing concentrations of dicoumarol, a known nitroreductase inhibitor (Figure 2f), thus confirming enzyme involvement. Probe **5b** conversion was also studied in presence of various other endogenous reducing agents, including reductases such as AzoR and NQO-1/2, as well as high concentrations of glutathione (GSH) representative of intracellular conditions (Figure 2g and Fig. S4). Only a slight fluorescence increase was detected in the presence of NQO-1 and NQO-2, which is consistent with their weak but known nitro-reducing activity reported in the literature.<sup>29</sup> Overall, these results support the selectivity of probe **5b** for NTR. Finally, UPLC-MS monitoring of the incubation of probe **5b** in the presence of NADH and NTR (Figure 2h) confirmed the release of **4-ANI** and revealed the transient formation of the corresponding hydroxylamine intermediate (**5b'**), validating the proposed two-step NTR-mediated activation mechanism. Together, these data validate

the functionality of the fluorogenic system designed for monitoring nitroreductase activity, demonstrating its ability to reliably track the enzymatic triggered release of an uncharged molecule. These promising results prompted us to pursue the study *in cellulo*, performing microscopy experiments.

### Confocal imaging assessment of SIS-mediated intramitochondrial delivery of uncharged amine compounds

The probes **5a-c** were incubated for 2 h with A549 cells at a concentration of 5  $\mu$ M and co-cultured in the presence of a mitochondrial near-infrared (NIR) marker.

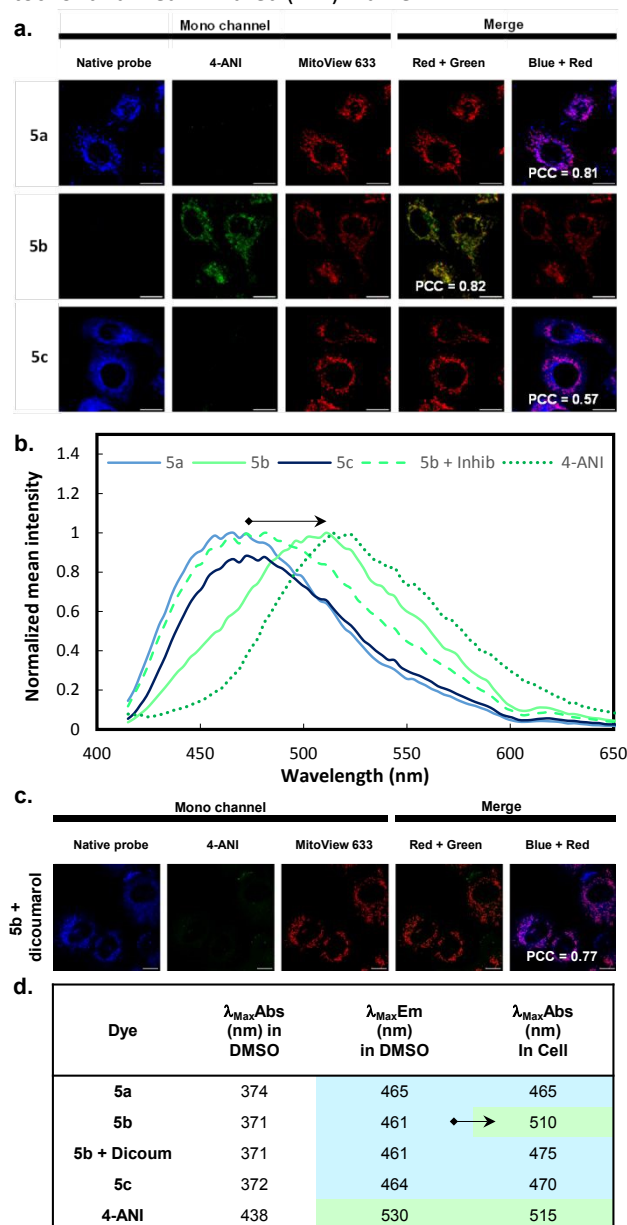


**Figure 3. Confocal microscopy.** **a.** A549 live cells were incubated for 3 h with probe **5a-c** at 5  $\mu$ M, then in the presence of MitoView 633 at 0.1  $\mu$ M for 15 min. Blue:  $\lambda_{\text{Exc}}$ : 405 nm,  $\lambda_{\text{Em}}$ : 415-450 nm; Green:  $\lambda_{\text{Exc}}$ : 440 nm,  $\lambda_{\text{Em}}$ : 500-550 nm. Red:  $\lambda_{\text{Exc}}$ : 630 nm,  $\lambda_{\text{Em}}$ : 650-750 nm. Pearson Correlation Coefficients (PCC) were calculated using using JACoP plugin of ImageJ. **b.** Emission spectra recorded *in cellulo* (Cf. Fig S4). **c.** A549 live cells were pre-incubated for 4 h with dicoumarol at 100  $\mu$ M then with probe **5b** at 5  $\mu$ M, and finally with MitoView 633 at 0.1  $\mu$ M for 15 min. Blue:  $\lambda_{\text{Exc}}$ : 405 nm,  $\lambda_{\text{Em}}$ : 415-450 nm; Green:  $\lambda_{\text{Exc}}$ : 440 nm,  $\lambda_{\text{Em}}$ : 500-550 nm. Red:  $\lambda_{\text{Exc}}$ : 630 nm,  $\lambda_{\text{Em}}$ :



650-750 nm. Pearson Correlation Coefficients (PCC) were calculated using JACoP plugin of ImageJ. **d.** Absorption and Emission maxima of probes **5a-c** in PBS buffer and estimated values in living cells.

Confocal microscopy imaging was performed in two separate channels, the settings being adjusted to give the best possible discrimination between the unactivated probe in blue and released **4-ANI** in green. As we can see in Figure 3a, only a blue emission was detected for probes **5a** and **5c**, indicating that no **4-ANI** release had occurred. In contrast, probe **5b** generated a distinct green signal, consistent with the release of **4-ANI**. TPP bearing probes **5a** and **5b** both displayed strong colocalization with this of the mitochondrial marker, as evidenced by Pearson correlation coefficients of 0.81 and 0.82, respectively. By comparison, detected signal upon probe **5c** incubation showed weak colocalization (Pearson coefficient = 0.57), confirming that this control compound, which lacks the mitochondrial targeting moiety, does not accumulate in mitochondria. These data demonstrate the necessity of combining both the mitochondriotropic group and the nitro-based activation trigger to achieve efficient mitochondrial delivery of uncharged amine-containing molecules such as **4-ANI**. To undoubtedly confirm this statement, in-cell emission spectra of the three probes were recorded following excitation at 405 nm and compared to that of free **4-ANI** (Figure 3b and Fig. S6). Probes **5a** and **5c** displayed emission maxima estimated at 465 nm and 470 nm respectively. In contrast, probe **5b** showed a red-shifted emission centered at 510 nm, closely matching the 515 nm peak observed for **4-ANI**, thereby confirming intra-mitochondrial release of the fluorophore. Furthermore, treatment with dicoumarol, a known nitroreductase inhibitor, suppressed the release, resulting in a shift of the emission peak back to 475 nm (Figure 3c-d). Finally, we recorded several images over time. While there is no doubt that the detected fluorescence upon probe **5b** incubation, attributed to the released **4-ANI**, was localized inside the mitochondria in the short time frame (Figure 3a), it progressively spread outside the mitochondria over time and was predominantly localized in the cytosol after 8 hours of incubation (Fig. S7). This result is consistent with the release of an uncharged molecule, which can therefore diffuse out of the mitochondria over time. Altogether, these results demonstrate that functionalizing the uncharged fluorophore **4-ANI** with the NTR-responsive, mitochondria-targeted SIS in probe **5b** enabled its efficient and selective shuttling through the cytosol to the mitochondria. To the best of our knowledge, this marks the first demonstration of a mitochondrial delivery strategy of uncharged molecule based on NTR mediated activation. We believe that this approach could be extended to a broad range of bioactive compounds, including therapeutic agents. To support this potential, we applied our system to achieve the mitochondrial shuttling of doxorubicin as a first proof of concept.

#### Mitochondrial shuttling of Doxorubicin using one-step functionalization with mitotargeted NTR activatable SIS

Prior studies, using covalent analogues of Doxorubicin, have demonstrated the real relevance of targeting this drug to the

mitochondria for the treatment of cancer, notably by limiting nuclear effects associated with cardiotoxicity, or to overcome specific resistance mechanisms.<sup>31</sup> In this context, we synthesized mito-targeted prodrugs of doxorubicin. Compounds **6a-c** were obtained in a single step through carbamoylation of the amine of **Dox** using nitrophenyl carbonates **3a-c** (Figure 4).

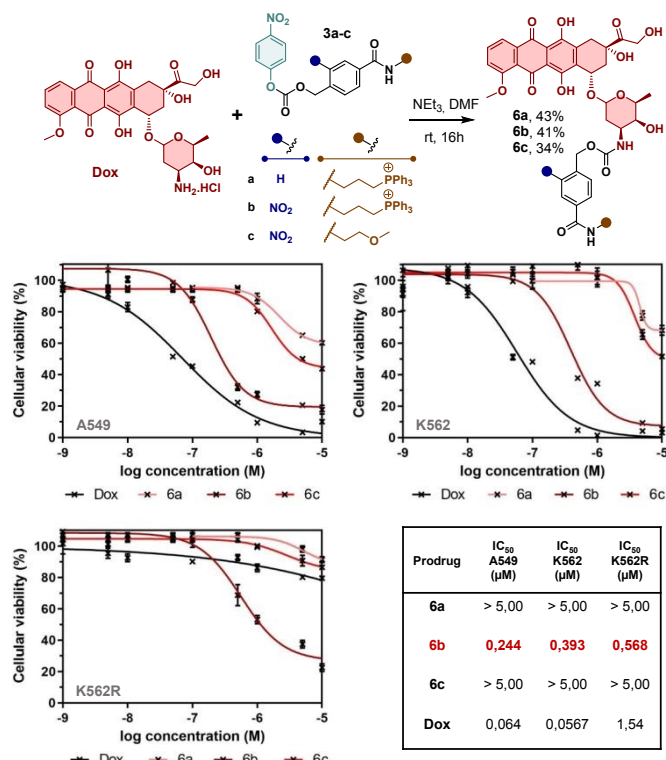


**Figure 4.** Cell viability studies in the presence of prodrugs **6a-c** and free **Doxorubicin**. Top: synthesis of prodrugs **6a-c**. Bottom: Evaluation of cytotoxic activities and IC<sub>50</sub> values resulting from cell viability assays performed on A549, K562 and K562r cell lines.

UPLC/MS analysis of prodrug **6b** after incubation with NTR for 2 hours confirmed the formation of free doxorubicin, along with the detection of a hydroxylamine intermediate and residual **6b**. These findings point to a slower enzymatic activation compared to probe **5b** (Figure S8), yet they demonstrate the functional integrity of the release system. Despite our attempts to visualize compounds **6a-c** by fluorescence microscopy, no detectable signal was observed, preventing subcellular localization analysis (Fig. S9). This limitation is most likely due to the poor intrinsic fluorescence properties of the prodrugs, as evidenced by their very low quantum yields (Fig. S10). To assess the biological relevance of this strategy, we performed a preliminary cytotoxicity study of both prodrugs **6a-c** and native doxorubicin (**Dox**) on three different cell lines: A549, K562, and doxorubicin-resistant K562r, overexpressing P-glycoprotein (PGP) pumps. Cytotoxicity was observed for both **Dox** and prodrug **6b** on A549 and K562 cells with IC<sub>50</sub> of 0.24 μM and 0.39 μM, respectively, for the latter, almost one order higher than **Dox** (Figure 4). In the meantime, neither compounds **6a** or **6c** displayed any significant toxicity (above 5 μM). These results



tend to support the requirement of both targeting and enzymatic activation, leading to intramitochondrial **Dox** release, for biological effect. More interestingly, while the activity of **Dox** was almost entirely lost on K562r, with IC50 rising from 0.056  $\mu\text{M}$  to 1.54  $\mu\text{M}$ , that of mitochondria-shuttled prodrug **6b** remained relatively constant at the submicromolar level. These results suggest that mitochondrial delivery using this mitotargeted NTR activatable SIS can bypass classical drug resistance mechanisms. Taken together, these data validate the potential of this mitochondrial shuttling strategy to enhance drug delivery, opening new avenues for its application beyond fluorophores to include therapeutic agents

## Conclusion

In summary, we report a straightforward and versatile strategy for the one-step functionalization of uncharged amine-containing molecules using a mitochondria-targeted, NTR-responsive self-immolative spacer (SIS). This approach enables efficient intracellular trafficking and selective mitochondrial delivery of uncharged amines, including both aliphatic and aromatic derivatives. The robustness of this system was first demonstrated both *in vitro* and *in cellulo* using fluorogenic probes based on the neutral dye **4-ANI**, confirming its stability, specificity, and enzymatic responsiveness. More importantly, we extended the concept to the mitochondrial delivery of doxorubicin, showing not only successful release but also preserved cytotoxic activity, even against drug-resistant cancer cells. These findings highlight the potential of this shuttling strategy to overcome resistance mechanisms commonly associated with chemotherapeutic failure. Overall, this technology represents a promising and adaptable platform for targeted mitochondrial delivery, with broad applicability in drug delivery, imaging, and therapeutic development.

## Author Contributions

Chemical synthesis Cell culture ex relating experiments including toxicity studies and confocal microscopy were performed by L. M. HPLC analysis and both chromatograms and spectra extractions for Figures were carried out with V. S. Treatment of kinetic data was performed by S. G-P. A. C. supervised the project and wrote the manuscript, with proof reading and suggestion given by P. D. All authors have given corrections and approval to the final version of the manuscript.

### Conflicts of interest

There are no conflicts to declare.

## Acknowledgements

This project has received funding by the French National Research Agency under the program ANR-21-CE18-0005-01 grant. We also thank the Institut de Chimie des Substances Naturelles for their financial support. The present work has

benefited from the Imagerie-Gif light microscopy core facility supported by the French National Research Agency (ANR-11-EQPX-0029/Morphoscope, ANR-10-INBS-04/FranceBioImaging; ANR-11-IDEX-0003-02/Saclay Plant Sciences). Laurie Askenatzis, Jérôme Bignon, H  l  ne L  vaique, and Emilie M  rour from the CIBI screening platform are acknowledged for their technical support. Universit   Paris-Saclay, and the CNRS are also acknowledged.

## Notes and references

1. a) X. Guo, N. Yang, W. Ji, H. Zhang, X. Dong, Z. Zhou, L. Li, H.-M. Shen, S. Q. Yao and W. Huang, *Adv. Mater.*, 2021, **33**, 2007778; b) M. P. Murphy and R. C. Hartley, *Nat. Rev. Drug. Discov.*, 2018, **17**, 865-886.
2. a) A. D. Scheid, T. C. Beadnell and D. R. Welch, *Br. J. Cancer*, 2021, **124**, 124-135; b) M. Golpich, E. Amini, Z. Mohamed, R. Azman Ali, N. Mohamed Ibrahim and A. Ahmadiani, *CNS Neurosci. Ther.*, 2017, **23**, 5-22; c) S. Vyas, E. Zaganjor and M. C. Haigis, *Cell*, 2016, **166**, 555-566; d) D. C. Wallace, *Nat. Rev. Cancer.*, 2012, **12**, 685-698; e) S. Fulda, L. Galluzzi and G. Kroemer, *Nat. Rev. Drug. Discov.*, 2010, **9**, 447-464.
3. a) M. M. Klemmensen, S. H. Borrowman, C. Pearce, B. Pyles and B. Chandra, *Neurotherapeutics*, 2024, **21**, e00292; b) G. Monzio Compagnoni, A. Di Fonzo, S. Corti, G. P. Comi, N. Bresolin and E. Masliah, *Mol. Neurobiol.*, 2020, **57**, 2959-2980; c) Y. Wang, E. Xu, P. R. Musich and F. Lin, *CNS Neurosci. Ther.*, 2019, **25**, 816-824; d) M. T. Lin and M. F. Beal, *Nature*, 2006, **443**, 787-795.
4. a) J. Szendroedi, E. Phielix and M. Roden, *Nat. Rev. Endocrinol.*, 2011, **8**, 92-103; b) B. L. Bradford and I. S. Gerald, *Science*, 2004, **303**, 1439-1439.
5. a) B. Fromenty and M. Roden, *J. Hepatol.*, 2023, **78**, 415-429; b) M. Myint, F. Oppedisano, V. De Giorgi, B.-M. Kim, F. M. Marincola, H. J. Alter and S. Nesci, *J. Transl. Med.*, 2023, **21**, 757; c) Y.-f. Li, Z.-f. Xie, Q. Song and J.-y. Li, *Acta Pharmacol. Sin.*, 2022, **43**, 1141-1155.
6. M. Cheng, D. Lu, K. Li, Y. Wang, X. Tong, X. Qi, C. Yan, K. Ji, J. Wang, W. Wang, H. Lv, X. Zhang, W. Kong, J. Zhang, J. Ma, K. Li, Y. Wang, J. Feng, P. Wei, Q. Li, C. Shen, X.-D. Fu, Y. Ma and X. Zhang, *Nat. Neurosci.*, 2025, **28**, 748-756.
7. a) R. A. J. Smith, C. M. Porteous, A. M. Gane and M. P. Murphy, *Proc. Natl. Acad. Sci. U.S.A.*, 2003, **100**, 5407-5412; b) M. P. Murphy, *Trends Biotechnol.*, 1997, **15**, 326-330.
8. S. Rin Jean, D. V. Tulumello, S. P. Wisnovsky, E. K. Lei, M. P. Pereira and S. O. Kelley, *ACS Chem. Biol.*, 2014, **9**, 323-333.
9. J. Zielonka, J. Joseph, A. Sikora, M. Hardy, O. Ouari, J. Vasquez-Vivar, G. Cheng, M. Lopez and B. Kalyanaraman, *Chem. Rev.*, 2017, **117**, 10043-10120.
10. H. Wang, B. Fang, B. Peng, L. Wang, Y. Xue, H. Bai, S. Lu, N. H. Voelcker, L. Li, L. Fu and W. Huang, *Front. Chem.*, 2021, **9**, 683220.
11. a) H. Crawford, M. Dimitriadis, J. Bassin, M. T. Cook, T. F. Abelha and J. Calvo-Castro, *Chem. Eur. J.*, 2022, **28**, e202202366; b) S. Samanta, Y. He, A. Sharma, J. Kim, W. Pan, Z. Yang, J. Li, W. Yan, L. Liu, J. Qu and J. S. Kim, *Chem*, 2019, **5**, 1697-1726; c) S. Wisnovsky, Eric K. Lei, Sae R. Jean and Shana O. Kelley, *Cell Chem. Biol.*, 2016, **23**, 917-927; d) Z. Xu and L. Xu, *Chem. Commun.*, 2016, **52**, 1094-1119; e)



- Roopa, N. Kumar, V. Bhalla and M. Kumar, *Chem. Commun.*, 2015, **51**, 15614-15628.
12. a) C. Ma, F. Xia and S. O. Kelley, *Bioconjugate Chem.*, 2020, **31**, 2650-2667; b) J. Y. Wang, J. Q. Li, Y. M. Xiao, B. Fu and Z. H. Qin, *ChemMedChem*, 2020, **15**, 404-410.
13. a) W. Zhang, G. Chen, Z. Chen, X. Yang, B. Zhang, S. Wang, Z. Li, Y. Yang, Y. Wu, Z. Liu and Z. Yu, *J. Control. Release*, 2024, **371**, 470-483; b) Y. Li, J. Liu, R. R. Weichselbaum and W. Lin, *Adv. Sci.*, 2024, **11**, 2403520; c) S. S. Liew, X. Qin, J. Zhou, L. Li, W. Huang and S. Q. Yao, *Angew. Chem. Int. Ed. Engl.*, 2021, **60**, 2232-2256; d) T. A. Tabish and M. R. Hamblin, *Biomater. Biosyst.*, 2021, **3**, 100023; e) W. Zhang, X. Hu, Q. Shen and D. Xing, *Nat. Commun.*, 2019, **10**, 1704.
14. R. Tiwari, P. S. Shinde, S. Sreedharan, A. K. Dey, K. A. Vallis, S. B. Mhaske, S. K. Pramanik and A. Das, *Chem. Sci.*, 2021, **12**, 2667-2673.
15. X. Luo, X. Gong, L. Su, H. Lin, Z. Yang, X. Yan and J. Gao, *Angew. Chem. Int. Ed. Engl.*, 2021, **60**, 1403-1410.
16. H.-W. Liu, X.-X. Hu, K. Li, Y. Liu, Q. Rong, L. Zhu, L. Yuan, F.-L. Qu, X.-B. Zhang and W. Tan, *Chem. Sci.*, 2017, **8**, 7689-7695.
17. A. Sharma, M.-G. Lee, H. Shi, M. Won, J. F. Arambula, J. L. Sessler, J. Y. Lee, S.-G. Chi and J. S. Kim, *Chem*, 2018, **4**, 2370-2383.
18. J.-n. Liu, W. Bu and J. Shi, *Chem. Rev.*, 2017, **117**, 6160-6224.
19. a) F. W. Hunter, B. G. Wouters and W. R. Wilson, *Br. J. Cancer*, 2016, **114**, 1071-1077; b) X. Yuan, Z. Xie and T. Zou, *Bioorganic Chemistry*, 2024, **144**, 107161.
20. a) P. Kameritsch, M. Singer, C. Nuernbergk, N. Rios, A. M. Reyes, K. Schmidt, J. Kirsch, H. Schneider, S. Müller, K. Pogoda, R. Cui, T. Kirchner, C. de Wit, B. Lange-Sperandio, U. Pohl, M. Conrad, R. Radi and H. Beck, *Proc. Natl. Acad. Sci. U.S.A.*, 2021, **118**, e1921828118; b) V. Scalcon, A. Bindoli and M. P. Rigobello, *Free Radic. Biol. Med.*, 2018, **127**, 62-79; c) F. Cabreiro, C. R. Picot, M. Perichon, J. Castel, B. Friguet and I. Petropoulos, *J. Biol. Chem.*, 2008, **283**, 16673-16681.
21. a) T. J. Mafireyi, J. O. Escobedo and R. M. Strongin, *Results Chem.*, 2021, **3**, 100127; b) H.-W. Liu, S. Xu, P. Wang, X.-X. Hu, J. Zhang, L. Yuan, X.-B. Zhang and W. Tan, *Chem. Commun.*, 2016, **52**, 12330-12333; c) M. H. Lee, J. H. Han, J. H. Lee, H. G. Choi, C. Kang and J. S. Kim, *J. Am. Chem. Soc.*, 2012, **134**, 17314-17319.
22. a) S. Wang, W. Tan, W. Lang, H. Qian, S. Guo, L. Zhu and J. Ge, *Anal. Chem.*, 2022, **94**, 7272-7277; b) M. Safir Filho, P. Dao, A. R. Martin and R. Benhida, *J. Photochem. Photobiol. A: Chem.*, 2020, **396**, 112528; c) N. Zhu, G. Xu, R. Wang, T. Zhu, J. Tan, X. Gu and C. Zhao, *Chem. Commun.*, 2020, **56**, 7761-7764; d) Z. Thiel and P. Rivera-Fuentes, *Angew. Chem. Int. Ed. Engl.*, 2019, **58**, 11474-11478; e) B. Huang, W. Chen, Y. Q. Kuang, W. Liu, X. J. Liu, L. J. Tang and J. H. Jiang, *Org. Biomol. Chem.*, 2017, **15**, 4383-4389; f) A. Chevalier, Y. Zhang, O. M. Khdour, J. B. Kaye and S. M. Hecht, *J. Am. Chem. Soc.*, 2016, **138**, 12009-12012.
23. a) Y. P. Yang, F. J. Qi, Y. P. Qian, X. Z. Bao, H. C. Zhang, B. Ma, F. Dai, S. X. Zhang and B. Zhou, *Anal. Chem.*, 2021, **93**, 2385-2393; b) Z. Yuan, M. Xu, T. Wu, X. Zhang, Y. Shen, U. Ernest, L. Gui, F. Wang, Q. He and H. Chen, *Talanta*, 2019, **198**, 323-329; c) W. S. Shin, M. G. Lee, P. Verwilt, J. H. Lee, S. G. Chi and J. S. Kim, *Chem. Sci.*, 2016, **7**, 6050-6059.
24. M. H. Xiang, H. Huang, X. J. Liu, Z. X. Tong, C. X. Zhang, F. Wang, R. Q. Yu and J. H. Jiang, *Anal. Chem.*, 2019, **91**, 5489-5493.
25. L. Michel, M. Auvray, L. Askenatzis, M.-A. Badet-Denisot, J. Bignon, P. Durand, F. Mahuteau-Betzer and A. Chevalier, *Anal. Chem.*, 2024, **96**, 1774-1780.
26. a) H. Xu, Y. Xiao, Y.-G. Liu and W. Sun, *Adv. Sensor Res.*, 2024, **3**, 2300032; b) C. Geraghty, C. Wynne and R. B. P. Elmes, *Coord. Chem. Rev.*, 2021, **437**, 213713.
27. a) W. Mao, X. Qian, J. Zhang, L. Xia and H. Xie, *ChemBioChem*, 2017, **18**, 1990-1994; b) Q. Jin, L. Feng, D.-D. Wang, Z.-R. Dai, P. Wang, L.-W. Zou, Z.-H. Liu, J.-Y. Wang, Y. Yu, G.-B. Ge, J.-N. Cui and L. Yang, *ACS Appl. Mater.*, 2015, **7**, 28474-28481; c) L. Dong, S. Shen, H. Lu, S. Jin and J. Zhang, *ACS Sensors*, 2019, **4**, 1222-1229.
28. C. Würth, M. Grabolle, J. Pauli, M. Spieles and U. Resch-Genger, *Nat. Protoc.*, 2013, **8**, 1535-1550.
29. R. J. Knox and S. Chen, in *Methods in Enzymology*, Academic Press, 2004, vol. 382, pp. 194-221.
30. S. R. Jean, D. V. Tulumello, C. Riganti, S. U. Liyanage, A. D. Schimmer and S. O. Kelley, *ACS Chem. Biol.*, 2015, **10**, 2007-2015.
31. a) J. Xi, M. Li, B. Jing, M. An, C. Yu, C. B. Pinnock, Y. Zhu, M. T. Lam and H. Liu, *ACS Appl. Mater.*, 2018, **10**, 43482-43492; b) W.-Q. Li, Z. Wang, S. Hao, H. He, Y. Wan, C. Zhu, L.-P. Sun, G. Cheng and S.-Y. Zheng, *ACS Appl. Mater.*, 2017, **9**, 16793-16802; c) Y. Zhang, C. Zhang, J. Chen, L. Liu, M. Hu, J. Li and H. Bi, *ACS Appl. Mater.*, 2017, **9**, 25152-25163; d) G. R. Chamberlain, D. V. Tulumello and S. O. Kelley, *ACS Chem. Biol.*, 2013, **8**, 1389-1395.



# A Mitochondria Targeted Nitroreductase-Sensitive Self-Immolative Spacer as Efficient Shuttle for Uncharged Amine-Based Molecules.

View Article Online

DOI: 10.1039/C5SC03665H

Laurane Michel,<sup>a</sup> Vincent Steinmetz,<sup>a</sup> Philippe Durand<sup>a</sup> and Arnaud Chevalier<sup>\*a</sup>

*a. Université Paris-Saclay, CNRS, Institut de Chimie des Substances Naturelles, UPR 2301, 91198, Gif-sur-Yvette, France.*

*E-mail:* arnaud.chevalier@cnrs.fr

## Data Availability Statement

The data supporting this article, including detailed synthetic protocols, additional figures, Absorbance and fluorescence spectra, NMR spectra and HRMS spectra, have been included as part of the Supplementary Information.

